

Unconventional Natural Gas Accumulations in Stacked Deposits: A Discussion of Upper Paleozoic Coal-Bearing Strata in the East Margin of the Ordos Basin, China



LI Yong^{1,2,*}, YANG Jianghao¹, PAN Zhejun³, MENG Shangzhi⁴, WANG Kai⁵ and NIU Xinlei¹

¹ College of Geoscience and Surveying Engineering, China University of Mining and Technology, Beijing 100083, China

² Shandong Provincial Key Laboratory of Depositional Mineralization & Sedimentary Minerals, Shandong University of Science and Technology, Qingdao 266590, Shandong, China

³ CSIRO Energy, Private Bag 10, Clayton South VIC 3169, Australia

⁴ China United Coal Bed Methane Co. Ltd, Beijing 100011, China

⁵ School of Earth and Space Sciences, Peking University, Beijing 100871, China

Abstract: The Upper Paleozoic (Carboniferous to Permian) succession in the east margin of the Ordos Basin in the North China Craton has a potential to contain significant hydrocarbon resources, though attention have been mainly attracted for its successful development of coalbed methane (CBM). To improve the previous resource estimates and evaluate the hydrocarbon play possibilities, this study incorporated new discoveries of hydrocarbon units and their stratigraphic relation with source rocks, hydrocarbon migration and trapping configurations. Continuous hydrocarbon accumulation units were identified within the Upper Paleozoic, including the Taiyuan, Shanxi and Xiashihezi formations with great tight gas potential, and the Taiyuan and Shanxi formations also containing shale gas and CBM. Different strata combinations are identified with coal deposition and favour for continuous gas accumulations, including the tidal flat, deltaic and fluvial systems distributed in most of the study areas. Methane was not only generated from the thick coal seams in the Taiyuan and Shanxi formations, but also from shale and dark mudstones. The coal, shale and tight sandstones are proved of remarkable gas content and hydrocarbon indications, and the gas saturation of tight sandstones decreases upward. The stacked deposit combinations vary isochronally in different areas, while the coal seams were developed stably showing good gas sources. Two key stages control the hydrocarbon enrichment, the continuous subsidence from coal forming to Late Triassic and the anomalous paleo-geothermal event happened in Early Cretaceous, as indicated by the fluid inclusions evidence. Extensive areas show good hydrocarbon development potential presently, and more works should be focused on the evaluation and selection of good reservoir combinations.

Key words: coal measure gas, transitional shale gas, tight sand gas, three gases, eastern Ordos Basin

Citation: Li et al., 2019. Unconventional Natural Gas Accumulations in Stacked Deposits: A Discussion of Upper Paleozoic Coal-Bearing Strata in the East Margin of the Ordos Basin, China. *Acta Geologica Sinica* (English Edition), 93(1): 111–129. DOI: 10.1111/1755-6724.13638

1 Introduction

Economic production of natural gas from coal seams (a.k.a. coalbed methane, or CBM) has been successfully achieved from the Upper Paleozoic in the Ordos Basin in north China, and significant amounts of CBM wells have been drilled (Yao et al., 2014; Zhang et al., 2014; Ma et al., 2016; Wang Tong et al., 2016; Li et al., 2017; Zou Caineng et al., 2018). Several noteworthy discoveries were made in the eastern-central Ordos Basin, including the Yulin, Sulige, and Daniudi gas fields, with the tight gas accumulated in Permian and Mesozoic extensively developed (Wang Zhenliang and Chen Heli, 2007; Hu et al., 2010; Xu et al., 2011; Yang et al., 2016; Wang et al., 2018; Wu et al., 2018). However, the Upper Carboniferous and Lower Permian succession was not the primary exploration target for sand gas, even though most of the CBM wells were drilled through the thick sandstones in

the Carboniferous Taiyuan and Permian Shanxi formations (Li et al., 2015; Kang Yongshang et al., 2017). Nevertheless, the presence of hydrocarbons was noted in many localities in the east margin of the Ordo Basin, and the properties of these potential tight gas reservoirs have been partly reported (Li et al., 2016).

The CBM resources in the whole Ordos Basin were estimated to be 3.5 trillion m³, and the in-situ tight gas resources are as much as 3.36 trillion m³. The tight gas accumulations in the inner part of the basin was considered as deep basin origin firstly, and now it is generally being accepted as stratigraphic lithologic type (Yang et al., 2005). During the extraction of CBM, gas traps in the sandstones near the coal reservoir have been discovered, for instance, 3 m thick sandstones above the coal being fractured showed production of 2400 m³/d in the Hancheng area and the production of tight gas interbedded with coal seams in the Piceance Basin (Johnson and Flores, 1998; Fall et al., 2014). A case study

* Corresponding author. E-mail: liyong@cumtb.edu.cn

discussing the natural gas accumulation in the Upper Paleozoic was firstly conducted in the Linxing area, with the natural gas accumulations showing different gas saturations from the lower coal bearing strata of Benxi and Taiyuan formations to the upon fluvial sandstones in Xiashihezi Formation (Li et al., 2016). However, the understandings of exploration of the tight gas in the whole study area are unresolved and incomplete. A few main questions require answers: (1) the capability of gas supplement from shale apart from the gas generated from coal, and furthermore if there is any development potential of the widely deposited marine to continental transitional shales; (2) the temporal and spatial evolution of hydrocarbon accumulations in the vast area (500 km length); and (3) the accumulation mechanism of different types of natural gases, and if there is any favorable strata combinations and etc.

Based on the recently acquired geological data from the whole study area, the source rock, reservoir units and their stratigraphic relationship to source rocks, trapping configuration, timing of hydrocarbon migration and preservation are considered in this study following the petroleum system analyses methods (Magoon and Dow, 1994; Galloway et al., 2016). The combination features of different kinds of unconventional natural gases was laid on focus, and the key factors controlling the hydrocarbon systems were discussed, following the methods in the literature (Gunter et al., 1997; Pashin, 2010; Tonnsen and Miskimins, 2010; Pan and Connell, 2012). The results will promote the tight gas, as well as shale gas, development in the vast coverage area of the east margin of the Ordos Basin.

2 Geological Setting

2.1 Geologic setting

The Ordos Basin is a tectono-sedimentary platform-type basin in the western part of the North China Craton (Fig. 1; Shuai et al., 2013; Jiao Yangquan et al., 2016; Zhao Wentao and Hou Guiting, 2017). It is also a large polycyclic cratonic basin that features monolithic vertical movement, the migration of depressions and simple constructions (Yang Minghui et al., 2010; Liao Jianbo et al., 2018; Han Hui et al., 2018). The CBM in the east margin of the Ordos Basin is primarily developed from the coal-bearing strata of the Carboniferous Taiyuan and Permian Shanxi Formations (Fig. 2). The Taiyuan Formation records lagoonal, tidal flat, and sandbar depositional environments in an epicontinental sea. Precursor coal vegetation was present in a tidal flat environment following a marine regression. The Shanxi Formation was deposited in a fluvial-deltaic environment with the precursor coal vegetation occurring in delta-plain deposits (Li et al., 2015). For better understanding the strata combinations and its CBM characteristics, the CBM target seams are classified into upper and lower coal seams, which represent the relatively thick CBM-producing seams in the lower part of the Shanxi Formation and in the middle-lower part of the Taiyuan Formation. The east margin of the Ordos Basin is primarily affected by tectonic movement from three directions: north of the Daqingshan orogenic belts, which resulted in the Yimeng

Uplift in the northern part of the basin, the southern part of the Qinling Orogenic Belt, which resulted in the Weibei Fold, and the eastern part of the Lvliang Mountain, which was named the Jinxi Fold in the study area (Yang et al., 2005; Fang Huihuang et al., 2017).

2.2 CBM development status

The proven CBM resources is approximately 1.2 trillion m^3 in the study area, and the proven technically recoverable CBM reserve is about 0.6 trillion m^3 (Li Yong et al., 2014). The CBM development blocks and areas can be classified into four parts based on their geological similarities: Hequ-Baode, Sanjiao-Liulin, Shilou-Linfen and Hancheng. The typical reservoir characteristics of the four areas are shown in Table 1. All CBM blocks show a broad variation in depth, generally from 400 to 1400 m and increasing from east to west. Deep CBM is also reported, for instance, CBM is produced from 2000 m deep coal seam in the Linxing area (Li et al., 2016). The main coal seams developed are classified as upper and lower coal groups as shown in Fig. 2. The burial depth of coal increases from the east to the west, with the elevation of the coal show a relatively stable variation trend (Figs. 3a and b). Moreover, the lower coal seams are thicker than the upper one, with a distance generally of 100 m between them (Figs. 3c and d). The coal roofs are generally composed of mudstones in the upper coal seam, whereas the roofs of the lower coal seams are mudstones, limestones and also sandstones. The permeability varies broadly due to the faults and small structures that are extensively developed in the whole east margin of the Ordos Basin (Table 1).

3 Methods and Database

The data of the basic coal characterization used in this paper, such as the coal thickness, maximum vitrinite reflectance ($\%R_{o, \max}$), coal burial depth and in situ gas content were collected from around 200 exploration wells (Fig. 1). These wells were drilled, and the data were collected and analysed by PetroChina and China United Coalbed Methane Co. Ltd. In addition, 15 sets of coal samples collected from the Xingwu Coal mines in Liulin area (centre of the eastern margin of Ordos Basin) were tested for their maceral compositions and pore-structure distributions. The well cross section and interpreted seismic section were also acquired for illustrating the stratigraphic combinations and gas occurrence characteristics. Based on these data, the characteristics of the unconventional natural gas geology conditions and their heterogeneity in the study area were analysed.

3.1 Coal, shale and sandstone reservoirs

Proximate analysis was performed following China National standards GB/T 212–1991. The $R_{o, \max}$ measurements and maceral analyses (500 points) were performed using a Leitz MPV-3 photometer microscope following the conventional methods according to China National Standards GB/T 6948–1998 and GB/T 8899–1998, respectively. Mercury porosimetry analyses were performed following Chinese Oil and Gas Industry



Fig. 1. Elementary structures in the east margin of the Ordos Basin and coalbed methane blocks distribution (modified from Li et al., 2017; China basemap after China National Bureau of Surveying and Mapping Geographical Information).

Standard SY/T 5346–1994 and using a Micromeritics 9310 Porosimeter, which automatically records the pressure, pore diameter, intrusion volume, and surface area. Before the porosimetric analysis, all samples were dried at 75 °C for 48 h. The specific surface area was determined by a

Micromeritics ASAP 2020 using N₂ adsorption/desorption at low temperature and pressures (77 K and <127 kPa) and the five-point BET method (Barrett, et al., 1951; Unsworth et al., 1989).

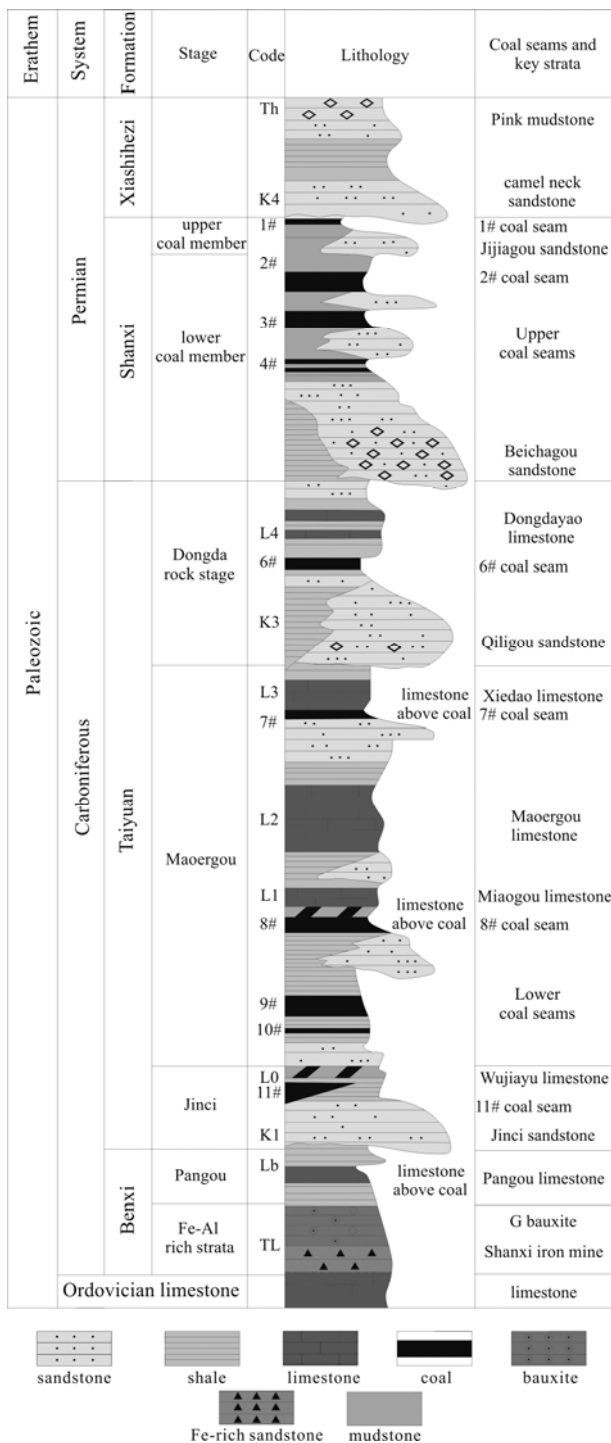


Fig. 2. Stratigraphic column of east margin of the Ordos Basin.

Table 1 Coal reservoir characteristics of typical CBM blocks in east margin of the Ordos Basin

Block	Hequ-Baode	Liulin-Sanjiao	Shilou-Linfen	Hancheng
Depth/m	300–1400	300–1100	800–1500	400–1300
U- $R_{0,max}$ (%)	0.57–0.78	1.43–1.49	1.39–1.94	1.6–2.20
L- $R_{0,max}$ (%)	0.53–0.81	1.65–1.75	1.45–1.97	1.6–2.20
U-Thickness(m)	5–10	5–9	5–8	3–10
L-Thickness (m)	5–14	5–8	5–10	4–10
U-gas content(m^3/t)	4–10	4–14	13–21	8–14
L-gas content(m^3/t)	4–12	4–13	9–20	6–14
U-roof	Mudstone	Mudstone	Mudstone	Mudstone
L-roof	Mudstone	Limestone	Limestone	Mudstone
Well test permeability ($\times 10^{-3} \mu m^2$)	2.5–8	0.01–10	0.01–40	0.22–3.5

U, Upper coal; L, Lower coal.

3.2 Gas content

The gas content of the coals was acquired following Chinese standard GB/T19559-2008, by testing desorbed gas for at least 8 hours, residual gas after crushing the coal to particles for at least 2 to 4 hours, and estimation of the lost gas (Bustin and Clarkson, 1998; Waechter et al., 2004). The isothermal adsorption experiments on the shales were conducted on fresh shale samples from the drilling cores, following Chinese Standard GB/T 19560-2004 at 30 °C.

3.3 Fluid inclusions

A Linkam THMS 600 heating and freezing table was used for fluid inclusions test at 20°C and 30% humidity. The fluid composition was measured by a LABHR-VIS LabRAM HR800 microscopic laser Raman spectroscopy. Both sandstone and limestone samples were collected from the occurrence layers deposited directly on coal seams. The fluid inclusions were mainly captured in the quartz overgrowths and sparry calcites, and the homogenous temperature and salinity was tested following the China Nuclear Industry Standards (EJ/T 1105–1999).

4 Results

4.1 Coal-bearing strata sequences

Two series of coal seams are developed in the study area, and the lower one (coal seam 8+9 in the Taiyuan Formation) are much more stable and thicker than the upper one (coal seam 3+4 in the Shanxi Formation). Another remarkable feature of the coal bearing strata is the thick and stable sandstone bodies largely developed: the Jinci sandstone located in the base of Taiyuan Formation (Fig. 4c), the Beichagou sandstone developed in the bottom of the Shanxi Formation (Fig. 4b), and the Luotuobozhi Sandstone in the bottom of the Xiashihezi Formation (Fig. 4a); moreover, there is the Qiaotou sandstones developed in the middle of the Taiyuan Formation (Wang Yue and Chen Shiyue, 2016). Limestones are primarily developed in the Taiyuan Formation and directly deposited upon the lower coal seams in the central part of the study area, and they have a direct influence on CBM preservation and production, resulting in higher water production in parts of the areas (Su et al., 2003; Lü et al., 2014; Li et al., 2015). Mudstones and shales are deposited mainly in a lagoon environment, where delta was developed, with sea water transgression of brachiopod fossils (Fig. 4d1) and higher plant leaf being observed (Fig. 4d2). Four typical

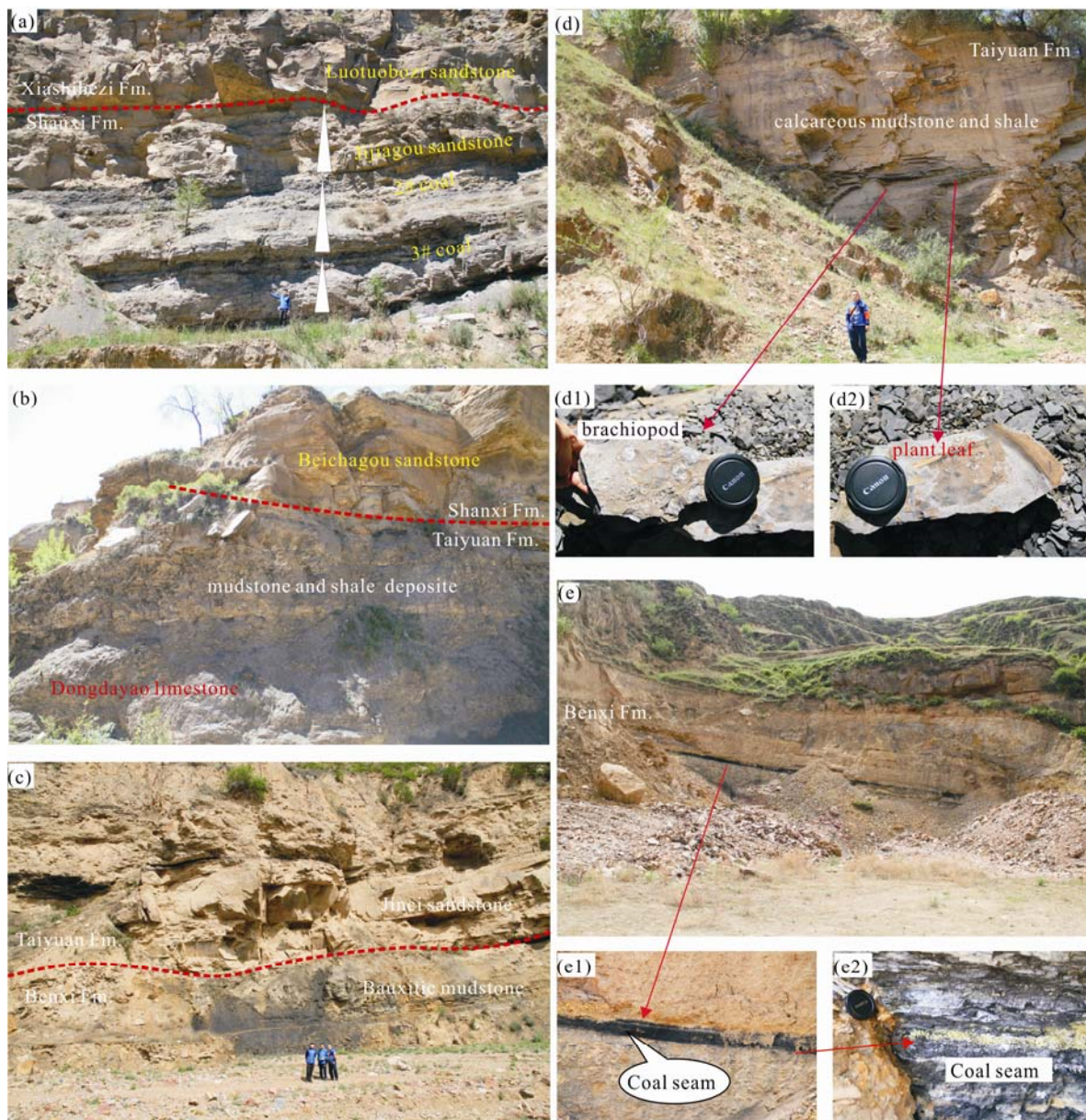


Fig. 4. Typical strata developed in the study area.

(a) Adjacent layers of the Shanxi and Xiashihezi formations, with the Shanxi Formation show three depositional cycle; (b) Stratigraphic boundary between Shanxi and Taiyuan formations, showing well developed mudstone/shale deposit and fluvial sandstones; (c) Taiyuan and Benxi formations boundary, showing thick Jinci sandstones; (d) Mudstone and shales deposited in the Taiyuan Formation, with brachiopod and higher plant fossils; (e) Thin coal seams occurred in Benxi Formation, showing high sulfur content.

combination of coal deposition series were observed from the well logs and drilling cores, including the tidal flat, deltaic, lake and fluvial depositional systems (Fig. 5).

4.2 Tidal flat depositional system

The main coal-accumulating environment of Taiyuan and Benxi formations is clastic coast deposit system with the influence of sea water transgression, and the coal seams generally show relatively high content of sulfur (Li et al., 2016). Accumulation of the main coal seams is intimately related to the slow rising of stratigraphic base level and corrective area of progradation. The coals were also deposited in shallow lagoon and peat swamp behind

barrier island where thick coal seams could be formed. However, in where calanque and tidal inlet channel developed, the coal seams were not stable horizontally. The depositional system is mainly observed in the Taiyuan Formation, showing variations to barrier and lagoon system during the sea level fluctuations (Li et al., 2015). In the early stage of Taiyuan Period, most plants grew in the water or moist ground, just like mangrove in recent period. Later along with regression, barrier island-lagoon and tidal flat deposition gradually developed. Due to the fluctuation of sea level, different coal series were deposited, and the advantageous environment of coal-forming was marsh area beside lagoon and tidal flat (Fig.

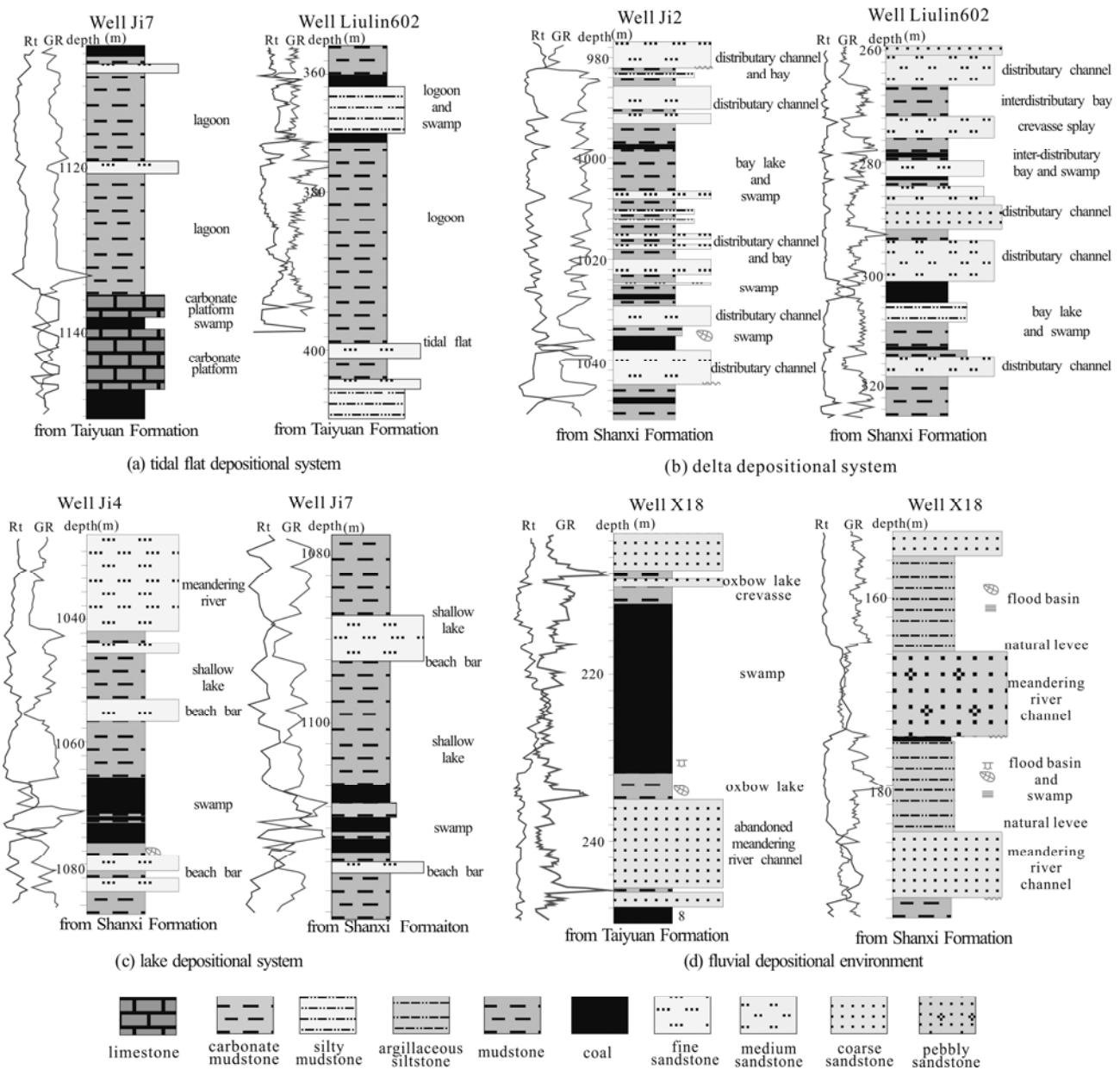


Fig. 5. Coal-bearing strata sequences in the study area.
(a) Tidal flat; (b) deltaic; (c) lake; (d) fluvial.

5a).

4.2.1 Deltaic depositional system

The deltaic depositional system was mainly deposited in the Shanxi Period. The main coal accumulating place was swamp behind coast in peat swamp microfacies of fluvial flood-plain, and the secondary coal accumulating place was abandoned channel swamp. The coal forming sequences are mainly started from distributary channels or distributary estuarine sand dam in delta plain, upward transited to inter distributary bays or flood basin facies, and then deposited in swamp or peat marshes. The roof of the upper coals is mainly deposited with marshes of distributary channels (Fig. 5b).

4.2.2 Lake depositional system

The shallow lake depositional systems mainly developed in the Jixian to Xiangning (located in south-central of the study area) in the lower of Shanxi Formation, occurred with large sets of gray mudstone deposits and grayish white sandstones. The coal forming strata are started from beach bar sandstones, upward to marsh mudstone and coal, and the coal seams are generally overlaid by mudstones, and partly by beach bar sandstones (Fig. 5c). The lake depositional system is relative limited compared with other depositional systems.

4.2.3 Fluvial depositional system

The vertical sequences of coal series developed in the

Table 2 Reservoir parameters from injection/falloff method of different blocks in east margin of the Ordos Basin, China (modified from Li Yong and Tang Dazhen, 2015)

Parameters	Linxing	Liulin	Shilou	Yanchuanan	Hancheng
Depth (m)	681–1071	488–1056	521–967	898–1290	532–1324
	879	740	849	1031	967
σ_{Hmin} (MPa)	10.0–20.8	5.8–20.9	11.2–20.8	9.0–21.8	10.3–31.8
	14.7	14.1	17.1	15.1	20.2
σ_{Hmax} (MPa)	11.6–32.8	10.1–33.3	18.6–32.6	16.1–53.8	9.8–33.3
	21.1	21.6	26.7	31.4	21.7
Reservoir pressure (MPa)	5.1–9.3	5.8–16.5	3.8–8.5	3.6–10.0	4.1–11.8
	7.5	13.1	7.1	5.8	7.8
Reservoir pressure gradient (MPa/100m)	0.75–0.91	0.41–1.12	0.71–0.95	0.39–0.86	0.48–1.0
	0.85	0.84	0.83	0.54	0.79
Reservoir temperature (°C)	19.6–20.1	19.6–35.1	24.3–42.3	31.5–45.4	21.5–43.0
	19.9	28.5	34.2	36.6	35.8
Permeability ($\times 10^{-3} \mu\text{m}^2$)	0.30–2.29	0.00–4.98	0.02–10.85	0.02–0.22	0.01–4.52
	1.07	0.46	1.56	0.10	0.65

Note: The three values are the (minimum–maximum)/average values. σ_{Hmin} =minimum principal stress; σ_{Hmax} =maximum principal stress.

fluvial system are mainly composed of channel demurrage deposits, beaches, natural levee, crevasse, and fining-upward marshes (Fig. 5d). Due to the influence of channel movement or migration, the thickness of coal seams varies (Fig. 3d), as shown in the Shanxi Formation. The fluvial deposition mainly occurred in the Xiashihezi Formation, and the fluvial channels are widely distributed with no coals being deposited.

4.3 Source rock potentials

Many indexes have been adopted to evaluate the thermal maturity of source rocks, including $R_{o, max}$, pyrolysis yield index, maximum pyrolysis temperature and hydrocarbon conversion index, of which the $R_{o, max}$ is the most commonly used and is adopted in this study (Sykes and Snowdon, 2002).

4.3.1 Thermal maturity of coal and shale

The $R_{o, max}$ of the upper coal seams varies between 0.59% and 2.39%, and the lower coal seams vary between 0.44% and 2.11%. The coals near Zijinshan Mountain show quite high values of $R_{o, max}$ due to the thermal event during Yanshanian Orogeny, with the $R_{o, max}$ values being higher than 4%. Generally, the $R_{o, max}$ values increase from north to south, and are higher in the west areas than in the east. The study area reached its deepest burial depth in Late Triassic, and during that time the burial depth was deeper in the south and shallower in the north (Wang Shuangming, 2011). In the Zhunger area, the $R_{o, max}$ varies in the range of 0.5%–0.65%, 0.59%–0.81% for the Fugu–Baode area, 1.23%–1.56% for the Liulin, 1.2%–1.7% for the Shilou and Daning areas, and 1.7%–2.6% for the Hancheng area.

In Table 3, the $R_{o, max}$ values of the shales were also measured, with the values varies between 0.82% and 1.61% for the samples (lack of relatively high thermal maturity samples from the southern areas like Hancheng), averaged at 1.30% (Fig. 6a). The thermal maturity variation of shales shows coincidence with coal, as the shales are generally interbedded within the coal seams of Shanxi and Taiyuan formations. The results show that most of the shales are in the mature stage, and the shales are of capacity in generating methane.

Table 3 Maceral composition and the thermal maturity of Upper Paleozoic shale and mudstones

Samples	Strata	Vitrinite (%)	Inertinite (%)	Liptinite (%)	$R_{o, max}$ (%)	TOC (%)
Sx1	Shanxi Formation	77.32	22.68	0	1.36	6.18
Sx2		78.99	21.01	0	1.38	8.53
Sx3		76.34	23.66	0	1.38	2.21
Sx4		74.28	25.72	0	1.38	3.97
Sx5		73.50	26.50	0	1.27	3.54
Sx6		73.70	26.30	0	1.59	1.12
Ty1	Taiyuan Formation	80.75	19.25	0	1.03	1.18
Ty2		78.30	21.70	0	0.87	2.44
Ty3		74.87	25.13	0	0.81	1.65
Ty4		75.56	24.44	0	1.47	3.95
Ty5		80.65	19.35	0	0.91	11.92
Ty6		83.30	16.70	0	1.77	2.17
Ty7		74.68	25.32	0	1.49	5.01
Ty8		63.60	36.40	0	1.51	1.14
Bx1	Benxi Formation	74.48	25.52	0	1.32	2.72
Bx2		68.89	22.01	9.1	0.91	1.77
Bx3		64.88	35.12	0	1.50	0.94

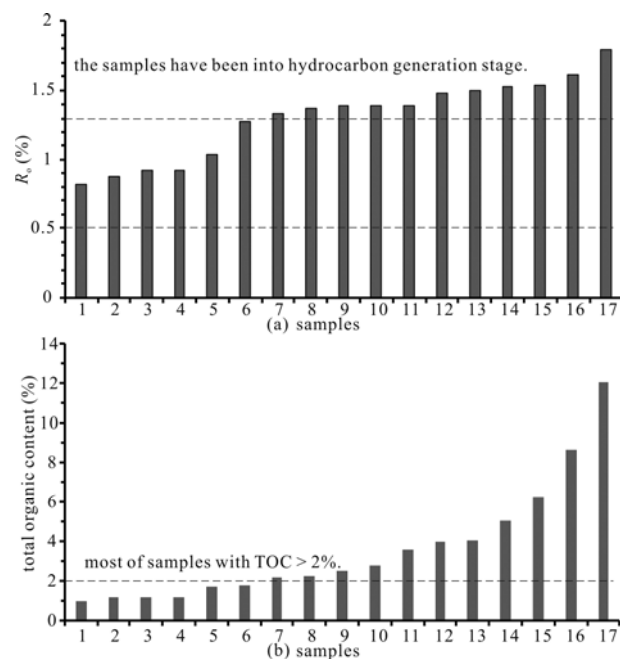


Fig. 6. Vitrinite reflectance variation and the total organic carbon contents of the shales in the east margin of Ordos Basin.

4.3.2 Source rock quality evaluation

Previous studies have shown that the coals would generate significant amount of CH₄ during its coalification process (e.g., Wang et al., 2015), and most of the gas would migrated to its adjacent strata with different gas saturations (e.g., Li et al., 2016). The coal would have provided enough gas for the Upper Paleozoic in most of the study areas, especially the middle and southern areas with $R_{o,max} > 1.2\%$, and thus put a solid hydrocarbon source foundation. As an important gas generating rock, the quality of shales is also discussed here.

The maceral compositions of the studied samples show that the shales are mainly composed of vitrinite, with the volume percentage from 65% to 85% of the organic matter, averaged at 76%. The inertinite content varies from 11% to 35% of the organic matter, with an average value of 23%. The liptinite is hardly seen from the tested samples (only two samples of low $R_{o,max}$ values), and the sapropelite is not observed. The calculated hydrocarbon indexes show that the shales are generally of type III kerogen. Combing the thermal maturity results of the shales (0.82% to 1.61%), the kerogen is in the main gas generation stage, showing that the shales are favorable for shale gas accumulations.

The TOC value is an important parameter for source rock quality (Hazra et al., 2016; Hakimi and Ahmed, 2016), and the TOC of the tested shale samples varies between 0.9% and 11.9%, with an average value of 3.6% (Fig. 6b). The results show that the shales are organic rich (generally accepted as TOC > 2%), which is favorable for gas generation.

4.4 Reservoirs

4.4.1 CBM reservoir

The Liulin area, which is famous for medium-volatile bituminous coal and is one of the first pioneer CBM areas in China, was chosen as a case study on the coal reservoir characteristics. The results of mercury intrusion and Brunauer–Emmett–Teller (BET) surface area using N₂ adsorption/desorption are plotted in Fig. 7. The results show that the porosity is quite limited, and the pores with are generally smaller than 10 nm. As for pores of different scales, the micro (0–10 nm) and transitional pores (10–100 nm) are dominant. No significant difference is shown in different sublayers by the two methods.

For a better explanation of the coal-reservoir characterization, the maceral group analysis and the proximate analysis of the samples sourced from the same coal cores are plotted in Fig. 8. Similar to the pore structure distribution results, the microscopic and element compositions of coal sublayers from shallow to deep show no significant difference. Thus, the differences in CBM reservoir and production characteristics are not mainly caused by the maceral composition difference and may be primarily due to the coal seam underground environment, structure positions, in situ stresses, and etc. (Bell, 2006; Li Yong et al., 2014; Flores, 2014).

4.4.2 Shale reservoir

The whole rock analysis show that the shales are mainly composed of clay minerals, and the secondary content is

terrigenous mineral clasts mainly of quartz with seldom K-feldspar and plagioclase (Table 4). The terrigenous content shows a volume content generally of 20% to 40%, with an average value of 31%. Carbonate minerals are hardly seen in the shale samples in the study area, with appearance in only 4 samples, mostly in the Taiyuan and Benxi formations, including calcite, dolomite and siderite. The carbonate was deposited during the transitional sedimentary environment, as transgressions were occurred commonly during the Taiyuan Formation. The pyrite is also generally observed in the tested samples, with an average content of 2.5% (values between 0.2% and 6.8%). The pyrite was generally deposited in a reduction condition, which means that the shale deposition is in a negative environment (Baioumy and Ismael, 2010).

Generally, the rock composition of the shale is clay minerals and quartz, with much higher content of clay minerals (generally > 50% in volume content), and the quartz is of an average value of 30%. The clay minerals contain significant content of micropores, which provide enough space for shale gas storage. It should be noted that the quartz content in the Shanxi Formation is higher than that in the Benxi and Taiyuan formations, while the pyrite content of the Taiyuan Formation is higher than the Shanxi Formation, which was caused by the terrestrial environment of the Upper Permian compared with epicontinental environment in the Taiyuan and Benxi periods (Li et al., 2015).

4.4.3 Tight sandstone reservoirs

Several thick sandstone layers are developed in the study area, especially in the north part, which has a good tight gas development potential with some areas been verified in the Linxing area. In Taiyuan and Shanxi formations, the Jinci, Qiaotou, and Beichagou sandstones are stably developed (Fig. 9; Figs. 4b and c), as well as the thick Luotuobozi sandstone bodies in the bottom of the Xiahihezi Formation (Fig. 4a). The sandstones acquired during well drilling were tested for helium porosity, with most of the porosity values varying between 0.35% and 22.29%, averaged at 7.65% (Fig. 10; Table 5). The

Table 4 Minerals composition of shales in east margin of the Ordos Basin

Samples	Qz	Kp	Pl	Cal	Dol	Aug	Sd	Py	Ana	Clay minerals
Sx1	4.40	/	/	/	/	/	/	0.2	/	95.4
Sx2	44.5	/	/	/	/	/	/	1.8	1.4	52.3
Sx3	30.1	/	1.1	/	/	/	7.1	1.1	/	60.6
Sx4	31.7	/	/	/	/	/	/	4.6	/	63.7
Sx5	33.4	/	/	/	/	/	/	0.4	0.9	65.3
Sx6	30.1	/	/	/	/	/	/	3.5	1.3	65.1
Ty1	32.8	/	/	/	/	/	/	5.4	1.5	60.3
Ty2	28.3	/	/	/	/	/	/	2.2	/	69.5
Ty3	23.2	/	/	/	/	/	/	1	1.2	74.6
Ty4	36.8	/	4.3	/	/	/	6.6	0.8	/	51.5
Ty5	22.5	/	/	/	/	/	/	2.6	1.5	73.2
Ty6	38.9	2.9	/	/	4.6	/	/	/	/	53.6
Ty7	30.8	/	/	6.4	1.8	/	/	1.1	/	59.9
Ty8	41.1	/	/	/	/	/	/	/	/	58.9
Bx1	26.3	/	/	/	/	/	/	3.1	/	70.6
Bx2	30.8	/	/	/	/	3.1	/	/	/	66.1
Bx3	30.0	/	/	/	/	/	/	6.8	1.5	61.7

Qz, Quartz; Kp, K-feldspar; Pl, Plagioclase; Cal, Calcite; Dol, Dolomite; Aug, Augite; Sd, Siderite; Py, Pyrite; Ana, Anatase.

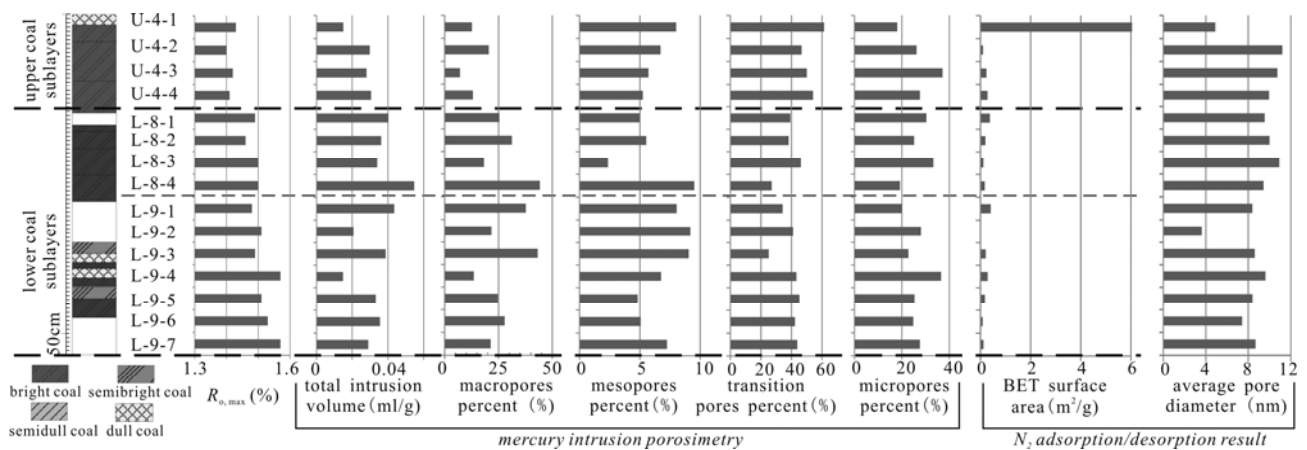


Fig. 7. Physical property of coal samples from sub-layers of the upper and lower coals in Liulin area, from top to bottom shows the sub-layers original sequence, mainly showing the mercury intrusion porosimetry and N_2 adsorption/desorption results.

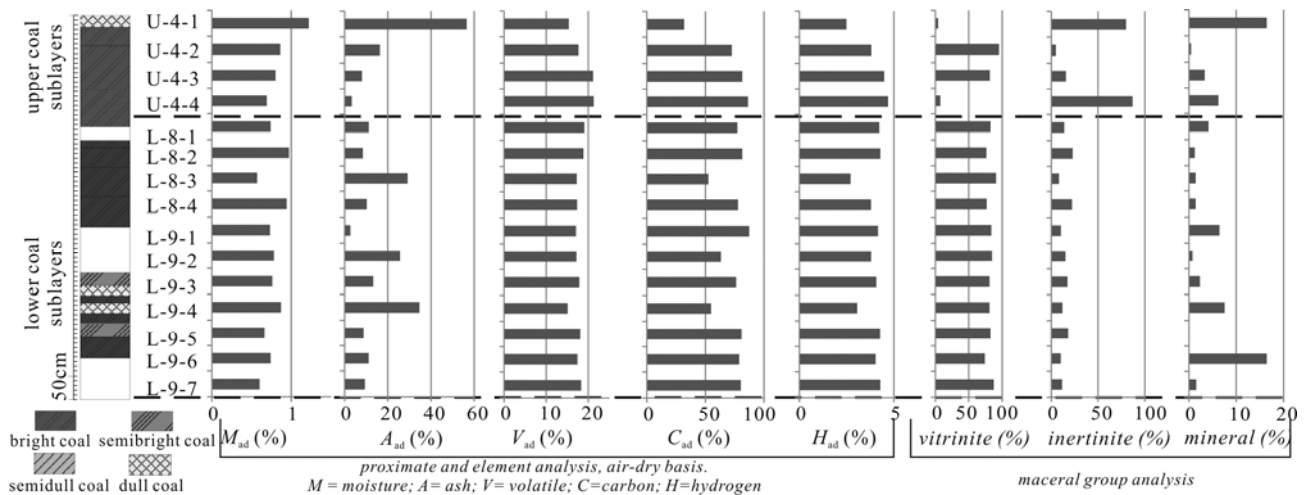


Fig. 8. Proximate analysis and maceral group analysis of coal samples from sub-layers of the upper and lower coals in Liulin area, from top to bottom shows the sub-layers original sequence.

Table 5 The distribution of porosity and permeability of different layers in the study area

Formation layers	Tested samples no.	Avg. porosity (%)	Avg. permeability ($\times 10^{-3} \mu\text{m}^2$)	Max. porosity (%)	Max. permeability ($\times 10^{-3} \mu\text{m}^2$)
He 8	437	6.25	0.23	21.81	4.06
Shan 1	115	5.34	0.1	13.64	1.22
Shan 2	214	5.63	0.26	11.0	8.29
Tai 1	173	7.48	0.19	13.19	1.55
Tai 2	875	7.28	0.46	14.1	11.09

average permeability of the samples is $0.72 \times 10^{-3} \mu\text{m}^2$, and quite a few samples being lower than $0.1 \times 10^{-3} \mu\text{m}^2$. The results show that the samples studied are generally tight sandstones, and same results have been reported by Li et al. (2016b).

4.5 Evidence of active continuous petroleum systems

For a better reflection of the gas accumulations in the whole Upper Paleozoic, the gas occurrence from coal, tight sandstones, and shales are studied below.

4.5.1 Gas content of coal

Most gas content is lower than $15 \text{ m}^3/\text{t}$, and the range of $5\text{--}15 \text{ m}^3/\text{t}$ is dominant in all the samples (Sanjiao–Liulin and Hancheng). The Shilou samples have the highest

values, which are higher than $15 \text{ m}^3/\text{t}$ due to their large burial depth of 1200–1500 m. The samples from the Hequ–Baode areas show the lowest range, mostly in the $0\text{--}5 \text{ m}^3/\text{t}$ range, which is generally caused by its low thermal maturity ($R_{o, \text{max}}$ ranges between 0.53% and 0.81%). With the increase of coal rank, the methane generation continuously increases with the rank ($R_{o, \text{max}}$ of 0.53% to 2.5%) of the study areas (Zhang et al., 2008; Pependic, 2011). The gas content of the tested samples generally shows an increase trend with coal rank, although the relationship is not linear (Li et al., 2016). The preservation condition is important for gas content, and the study areas is of different geology and hydrogeology condition which has a direct influence on the gas content (Li et al., 2015). Thus, the gas content is mainly controlled by the coal rank

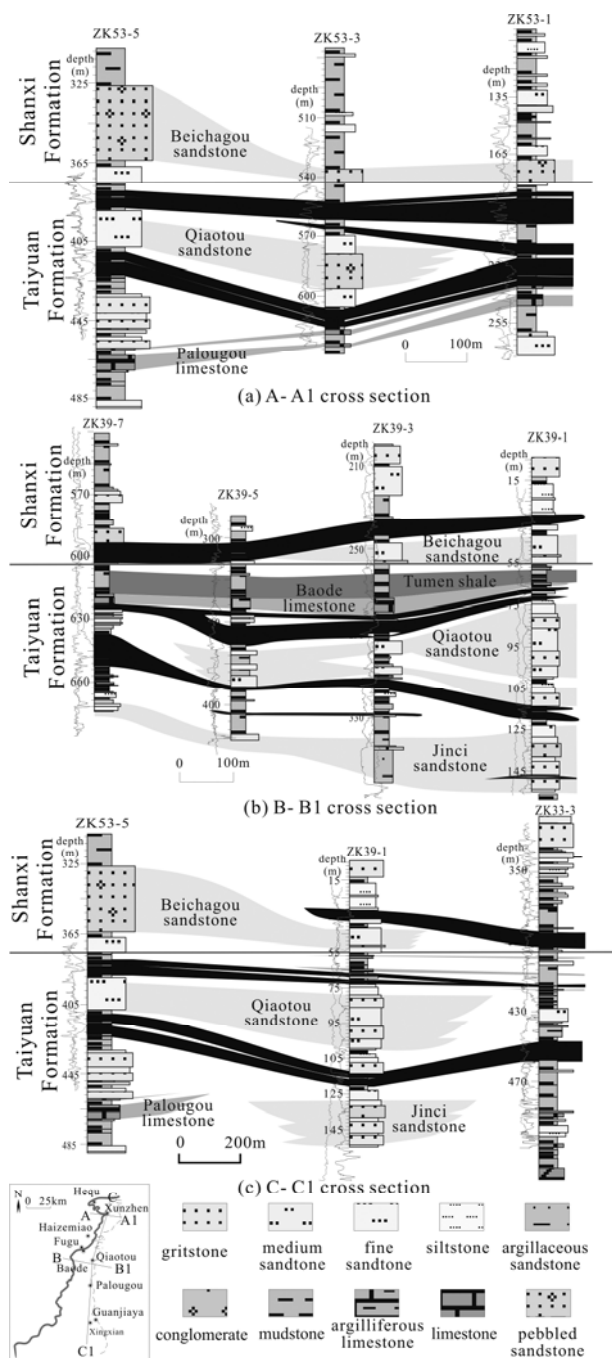


Fig. 9. Well cross-section showing the strata combinations of the study area.

and sealing conditions of the CBM reservoirs.

4.5.2 Gas content of shale

Isothermal adsorption experiments were conducted on sampled shales, and adsorbed gas content were calculated based on the initial reservoir pressure (Table 6). The adsorbed gas content varies between 0.2 and 2.0 m³/t, and is 0.67 m³/t on average. Furthermore, the gas content shows a positive relationship with TOC value (Fig. 11), mainly of two reasons: (1) the higher TOC values generally mean higher gas generation potential; and (2) the

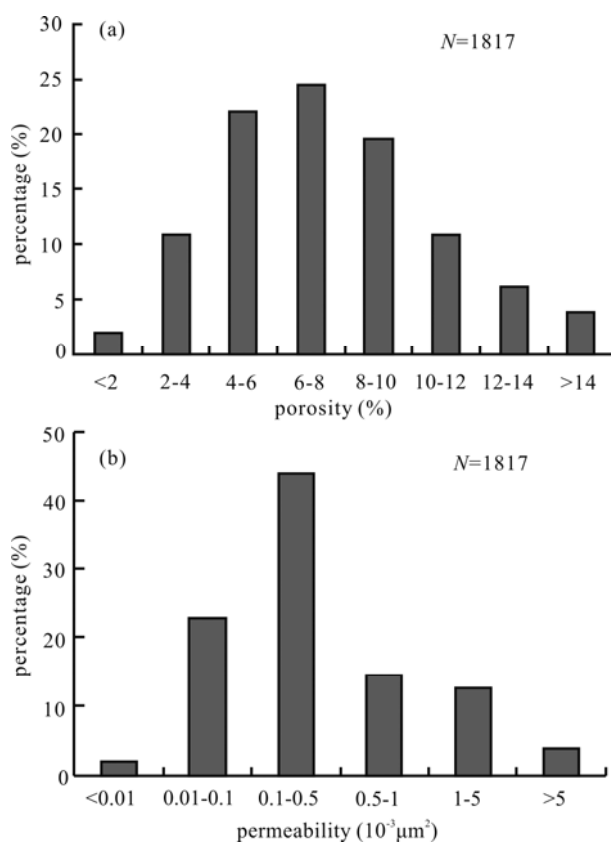


Fig. 10. Distribution of porosity and permeabilities of sandstones in the study area.

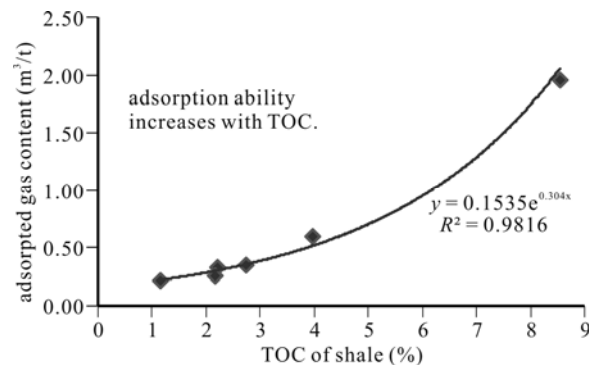


Fig. 11. Relationship between TOC and adsorbed gas content of shales in the study area.

Table 6 Adsorbed gas content at reservoir pressure (*V*) of shale (30°C)

Samples	V_L (m ³ /t)	P_L (MPa)	V (m ³ /t)
1-1	2.18	1.64	1.96
1-2	0.36	1.19	0.33
2-1	0.64	1.21	0.60
2-2	0.27	0.74	0.25
2-3	0.23	0.94	0.21

V_L , Langmuir volume; P_L , Langmuir pressure.

kerogen is generally of largely developed micropores, which means higher adsorption ability to gas; meantime, gas hydrocarbons are easily dissolved in the amorphous and unstructured matrix asphalts. Thus, higher TOC value generally means higher gas generation potential and

adsorption ability.

4.5.3 Gas occurrence in tight sandstone

Except for the successfully developed tight gas wells located in the Linxing area, tight gas layers were interpreted during the CBM wells drilling in most of the study area. The presented well is in the Linfen, south of the study area. It can be seen that different types of layers all show good hydrocarbon accumulation (Fig. 12). Two sandstone layers found in each of the Shanxi and Taiyuan Formations, with the mudstones/shale gas bearing layers also found. The most successfully developed gas layer in the He 8 member of the Xiashihezi Formation in the central and eastern Ordos Basin (Yang Hua et al., 2012). Recently the exploration results show that the gas layers in the Shanxi and Taiyuan formations could be a good gas supplement (Li et al., 2016), which is significant in clearly knowing the gas potential in the whole east margin of the Ordos Basin and its economic efficiency for co-production

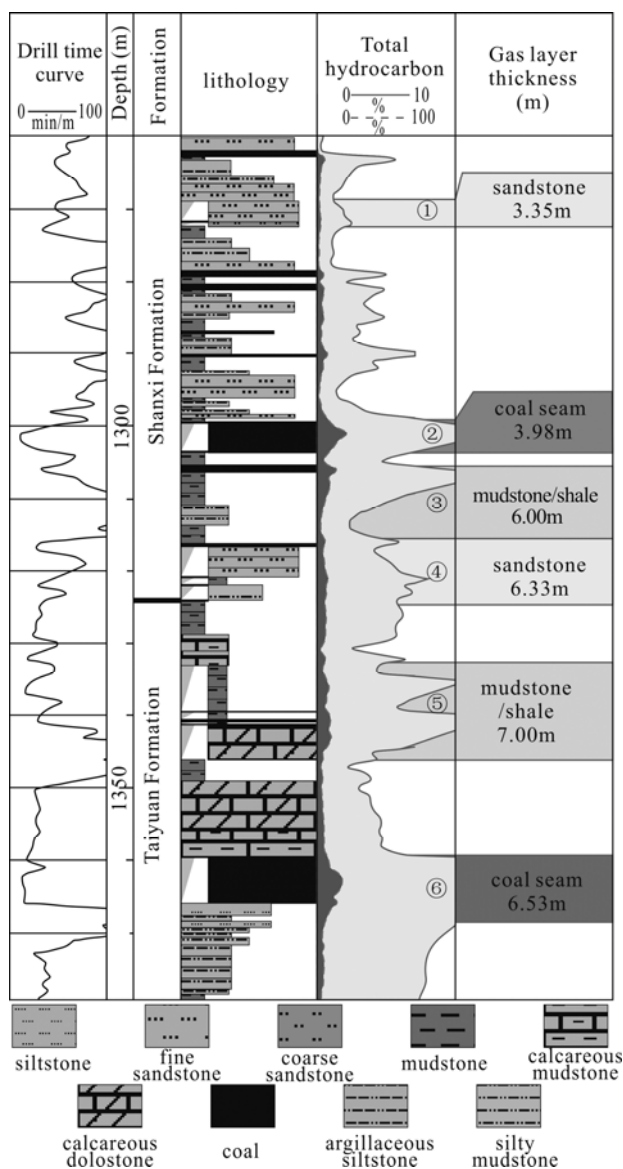


Fig. 12. Gas layers observed in the Shanxi and Taiyuan formations, with six interpreted layers.

from one well (Meng et al., 2018).

5 Discussions

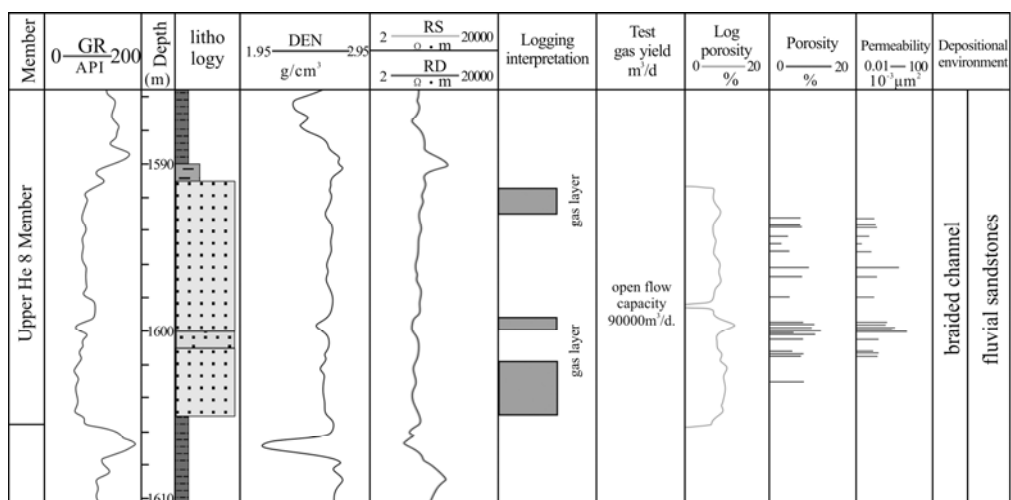
5.1 Favourable strata combinations

Comparing the different coal depositional series, the fluvial sandstones (Fig. 13a), distributary sandstones deposited in the delta system (Fig. 13b), and the barrier sandstones (Fig. 13c) all show gas development potential. The interpreted and tested gas layers are sealed by the overlying and underlying mudstones. The tested porosity and permeability for the sandstone cores show poor reservoir quality, and the gas layers in Shanxi and Taiyuan formations are much deeper than that of Xiashihezi Formation. From low to the up strata, the gas saturation and reservoir pressure decrease gradually due to that the source rocks are mainly the coal and mudstones in the Taiyuan and Shanxi formations (Li et al., 2016). From the basin edge to center (Fig. 3b), the burial depth increases and this is more favorable for tight gas and shale gas accumulation than the basin edge (Fig. 14). As the CBM was generally developed from the shallow buried coal seams, the east areas are more suitable for CBM production with better permeability than the deep buried coal seams in the west (Li et al., 2017).

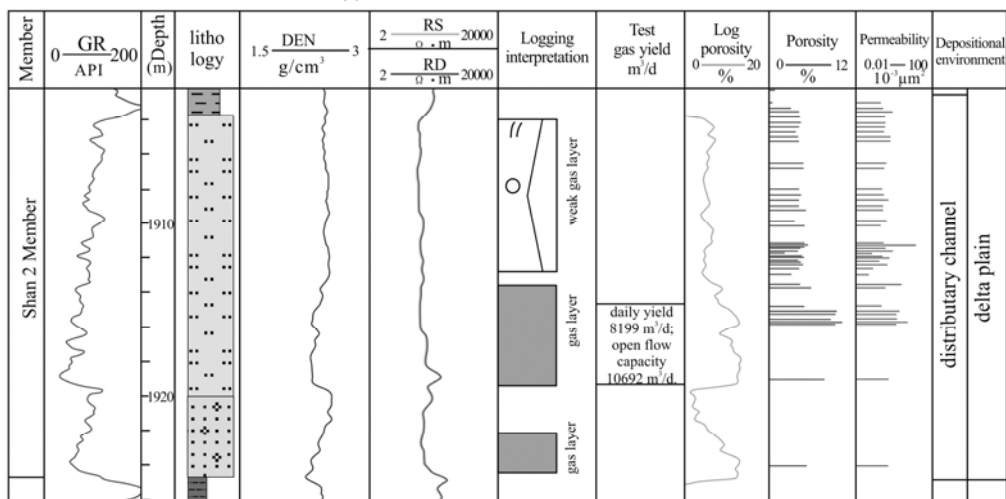
From south to north, the sedimentary environments both of Taiyuan and Shanxi formations show great variations (Fig. 15). As for the Taiyuan Formation, the sedimentary facies vary from tidal flat in the south, to the neritic shelf and lagoon systems in the center areas, and then transit to the tidal flat and delta plain in the north. The Shanxi Formation shows a variation from delta front to shore-shallow lake, delta plain and front, and then fluvial and flood plain, and the fans and braided rivers. For an efficient hydrocarbon accumulation, strong gas supplement and good reservoirs are both necessary, thus, where relative thick coal and sandstone deposited, combing mudstones as seal, would be potential development target. As for Shanxi Formation, all the east margin of the Ordos Basin may be good choice, and for sandstone in the Taiyuan Formation, the Hancheng to Jixian area and the Sanjiao to Zhunger areas may have potential. Furthermore, as the Benxi Formation was also deposited with several coal seams, thus sandstones underlying the coal seams in the Taiyuan Formation are also attractive, especially in the south areas with relatively high coal maturity.

5.2 Key stages controlling hydrocarbon migration and accumulation

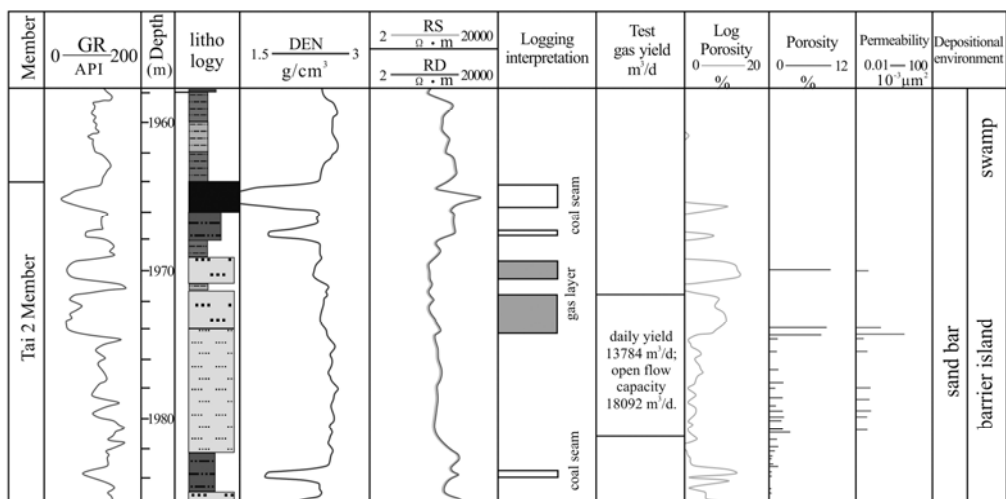
The thermal evolution history from north to south was studied, and the results show that hydrocarbon generation happened in two stages: (1) the continuous subsidence from coal forming to the Hercynian period in Late Triassic; and (2) the anomalous paleo-geothermal field happened in the middle Yanshanian period from Late Jurassic to Early Cretaceous (Fig. 16; Li et al., 2016; Xu et al., 2015; Ma et al., 2016). It should be noticed that the north areas (Fig. 16a) show a continuous subsidence from deposition to Late Cretaceous, however, three stages of fluid inclusion were detected, and the maximum burial



(a) section from Xiashihezi Formation



(b) section from Shanxi Formation



(c) section from Taiyuan Formation



Fig. 13. Tight gas accumulations in different formations of the reservoirs. (a) Xiashihezi Formation; (b) Shanxi Formation; (c) Taiyuan Formation.

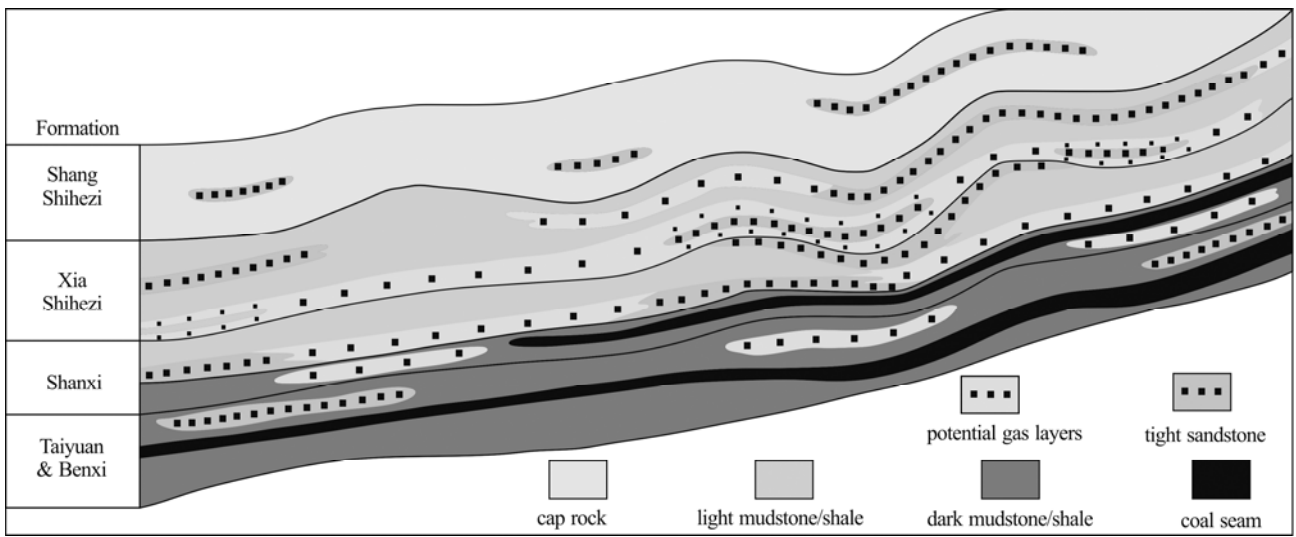


Fig. 14. Simplified reservoir combinations of coal, shale, mudstones in the east margin of the Ordos Basin.

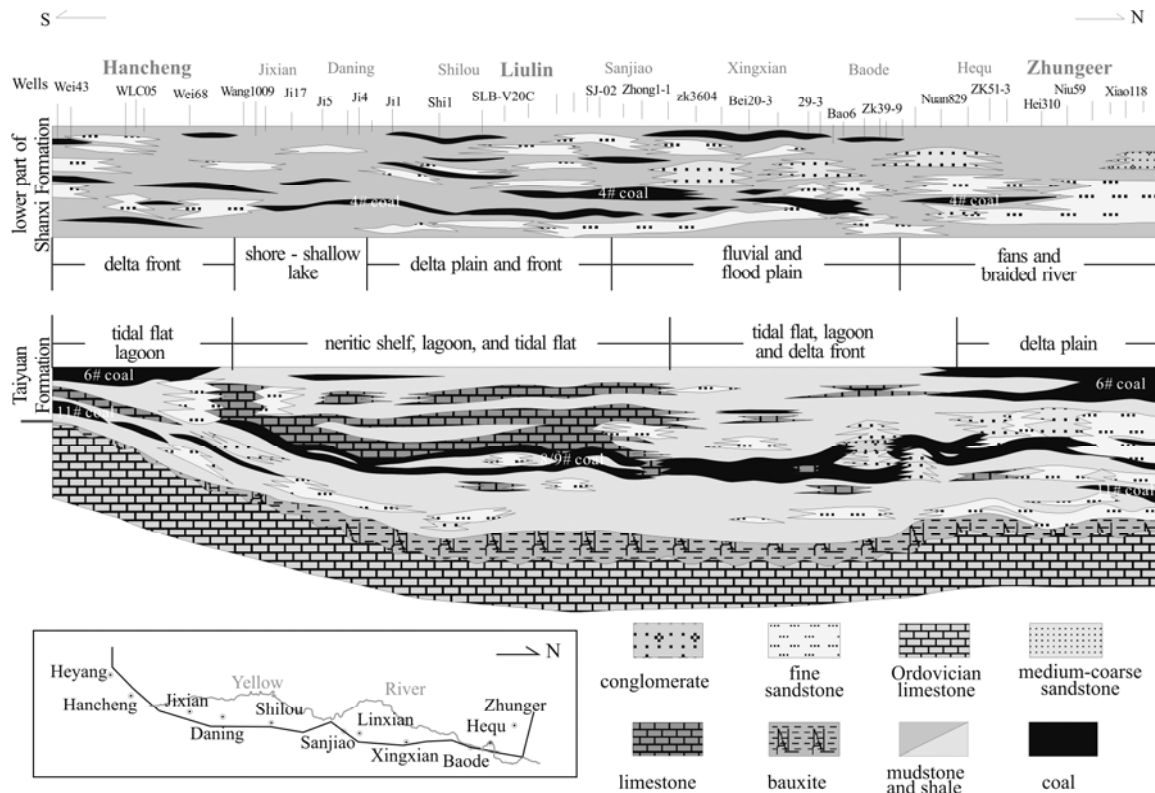


Fig. 15. Well cross-section from the south to the north of Taiyuan and lower part of the Shanxi formations (modified from Ouyang et al., 2018).

temperature was also influenced by abnormal thermal event (Xu et al., 2015). The homogeneous temperature and salinity measurements of sample from the Liulin areas (located in the centre of the study area) verified that two stages of hydrocarbon generation and migration occurred (Fig. 17). The fluid inclusions developed along quartz overgrowths of different stages and microfractures in Shanxi Formation (Figs. 18a and b), and also occurred in recrystallized calcites (Figs. 18c and d) in Taiyuan Formation. The yellow to green fluorescence shown in the

hydrocarbon migration channels and where hydrocarbon was captured (Figs. 18e to h).

Another phenomenon should be noted is that the maximum burial depth of the source rocks in the south areas (with $R_{o, \max}$ around 2.0%) is shallower than that in the north ($R_{o, \max}$ around 1.0%) and centre areas ($R_{o, \max} > 1.3\%$). The terrestrial heat flow in the south was higher than that in the centre and north areas, which substantially influence the thermal evolution and also gas content in coals.

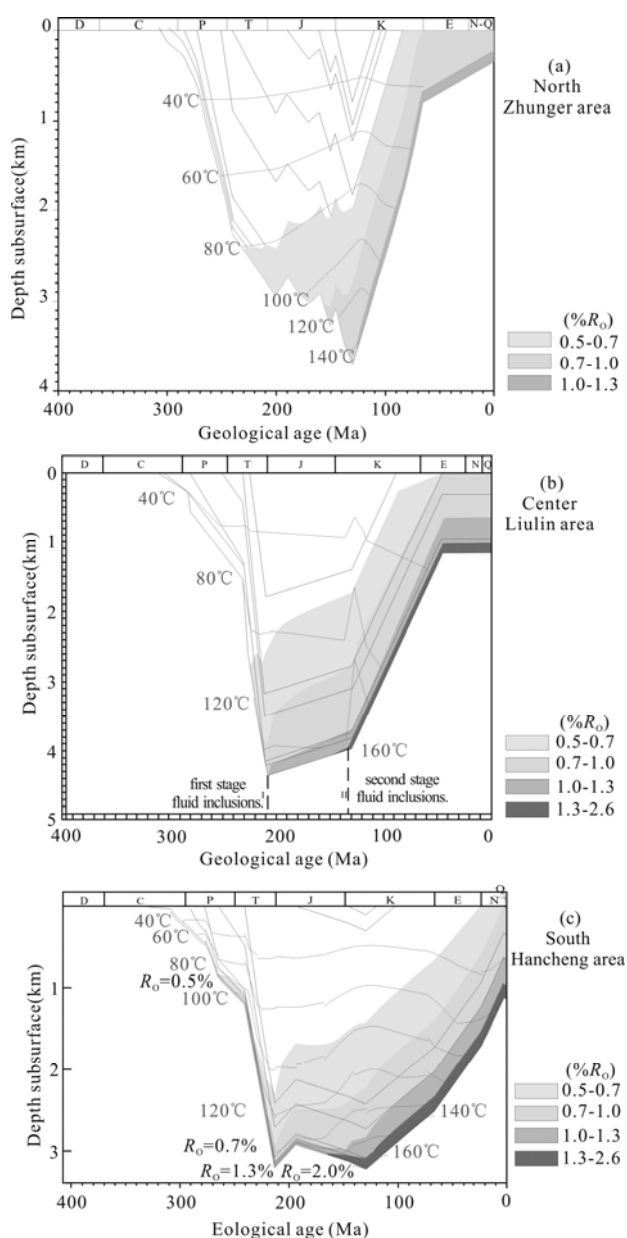


Fig. 16. Thermal evolution history from north to south in the study area, with figure (a) referred to Xu et al., 2016; figure (c) referred to Ma et al., 2017.

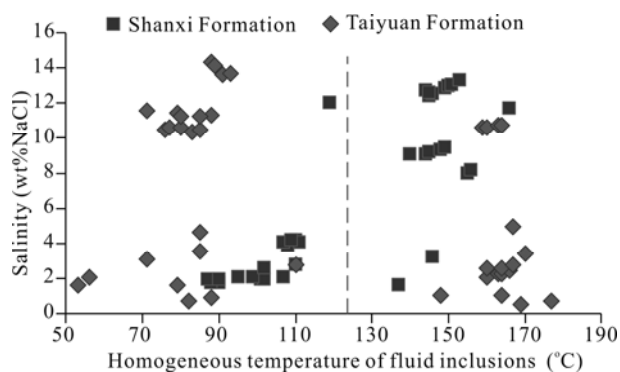


Fig. 17. Homogeneous temperature and salinity relationship of the tested fluid inclusions from the Shanxi and Taiyuan formations.

As shown above, the source rock reached its peak gas generation stage during the Late Jurassic to Early Cretaceous, during which the gas may breakthrough the overlying strata upon coals and mudstones. The migrated gases were mainly preserved in lithological reservoirs in form of tight gas (Li et al., 2016). After the Cenozoic, the basin was continuously being uplifted, and gases in coal desorbed and gases in sandstones were de-pressurized with part of the gas being released. The strata uplifted in the late stage, not only resulted in gas migration of the upper strata, but also made former tightly preserved CH_4 migrated from coal and shales, and being re-trapped in the upper coal, shale and tight sandstones, as recognized from the isotope values of $\delta^{13}\text{C}_{\text{CH}_4}$ (Li Yong et al., 2014; Fig. 19). The Upper Palaeozoic developed two sets of source rocks, the coal and dark mudstones in Taiyuan and Shanxi Formations. The coal has been proved of much higher hydrocarbon generation ability and contribution than mudstone and shales (Hunt 1991; Gong et al., 2018). The gas saturation decreases as with the increase of reservoir distance with the coal seams (Figs. 20a and b).

The study area was influenced by two stages of tectonic movement after the deposition of coal measures, the Yanshannian orogeny in NW-SE direction and the Himalayan Orogeny in NEE-SWW direction, resulted in orthogonal joints cutting the strata in vertical (Fig. 20c; Gao et al., 2018). The movement also resulted in the channel for gas migration from the lower to the upper strata, which was good for the gas accumulation in the Xiashihezi Formation and its upper strata (Fig. 19).

6 Conclusions

(1) Stacked hydrocarbon accumulation units were identified within the Upper Paleozoic, with the Taiyuan, Shanxi and Xiashihezi formations are of great tight gas development potential, and the Benxi, Taiyuan and Shanxi formations contain transitional shale gas, apart from the already commercially developed CBM.

(2) Four strata combinations were identified with coal deposition and favor for continuous gas accumulations, the tidal flat, deltaic and fluvial systems, which vary from Taiyuan to Shanxi and Xiashihezi formation, located in most of the study area, and the lake depositional environment mainly located in the southern part.

(3) The methane was not only generated from the thick coal seams in Taiyuan and Shanxi formations, but also from shale and dark mudstones. The coal, shale and tight sandstones are proved of remarkable gas content and hydrocarbon indications, even though the reservoir quality varies between different formations and even within one single layer.

(4) Two key stages controlled the hydrocarbon enrichment, the continuous subsidence from coal forming to Late Triassic and the anomalous paleo-geothermal event happened in Early Cretaceous. The Yanshannian and Himalayan tectonic movements resulted in vertical joints and faults to connect the Paleozoic strata, leading to gas migration and accumulation. The stacked deposits in the study area vary laterally and also vertically, and extensive areas show good hydrocarbon development potential.

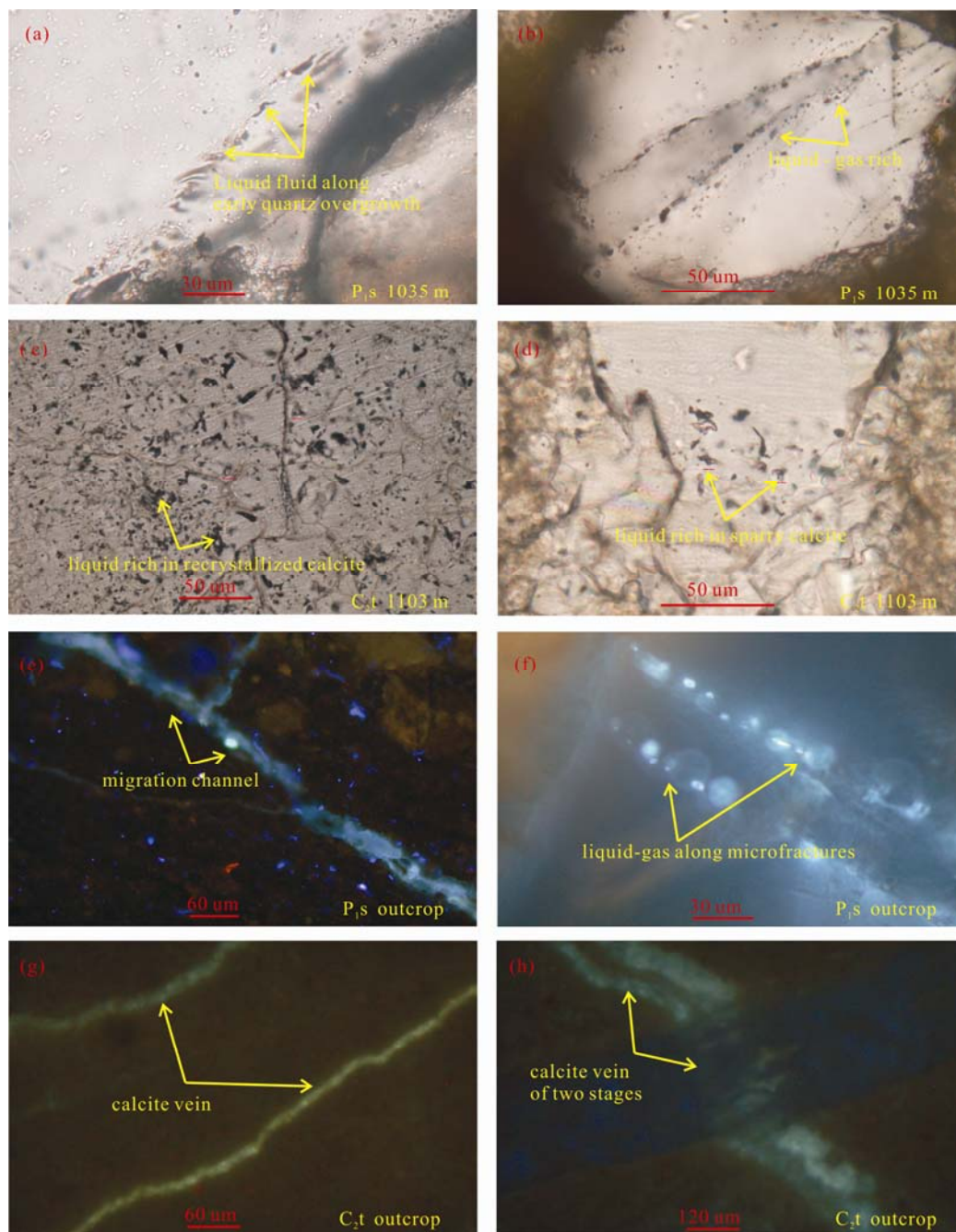


Fig. 18. Fluid inclusions in the study area.

(a) taupe gray liquid fluid trapped along quartz overgrowths developed in early stages, sample from Shanxi Formation; (b) taupe gray and gray liquid, liquid-gas fluid, and gas fluid trapped in quartz overgrowths and microfractures, sample from Taiyuan Formation; (c) liquid, liquid-gas, hydrocarbon-containing saline inclusions trapped along recrystallized calcite of early stages, sample from Shanxi Formation; (d) liquid and saline fluid inclusion occurred along fractures in sparry calcites, sample from Taiyuan Formation; (e) yellow to green fluorescence in microfractures of sandstones, shown as hydrocarbon migration channel, sample from Shanxi Formation; (f) yellow to gray gas-liquid inclusion developed along quartz microfractures; (g) light yellow fluorescence occurred in calcite veins; (h) two stages of calcite vein occurred, the former one show light yellow fluorescence.

More works should be focused on the evaluation and selection of good reservoir combinations.

Acknowledgments

This work was supported by the Natural Science

Foundation of China (grant No. 41702171), the Beijing Municipal Excellent Talents Foundation (grant No. 2017000020124G107), 2017 Open Project Fund of State Key Laboratory of Coal Resources and Safe Mining (grant No. SKLCRSM17KFA12) and the Joint Research Fund for Overseas Chinese Scholars and Scholars in Hong

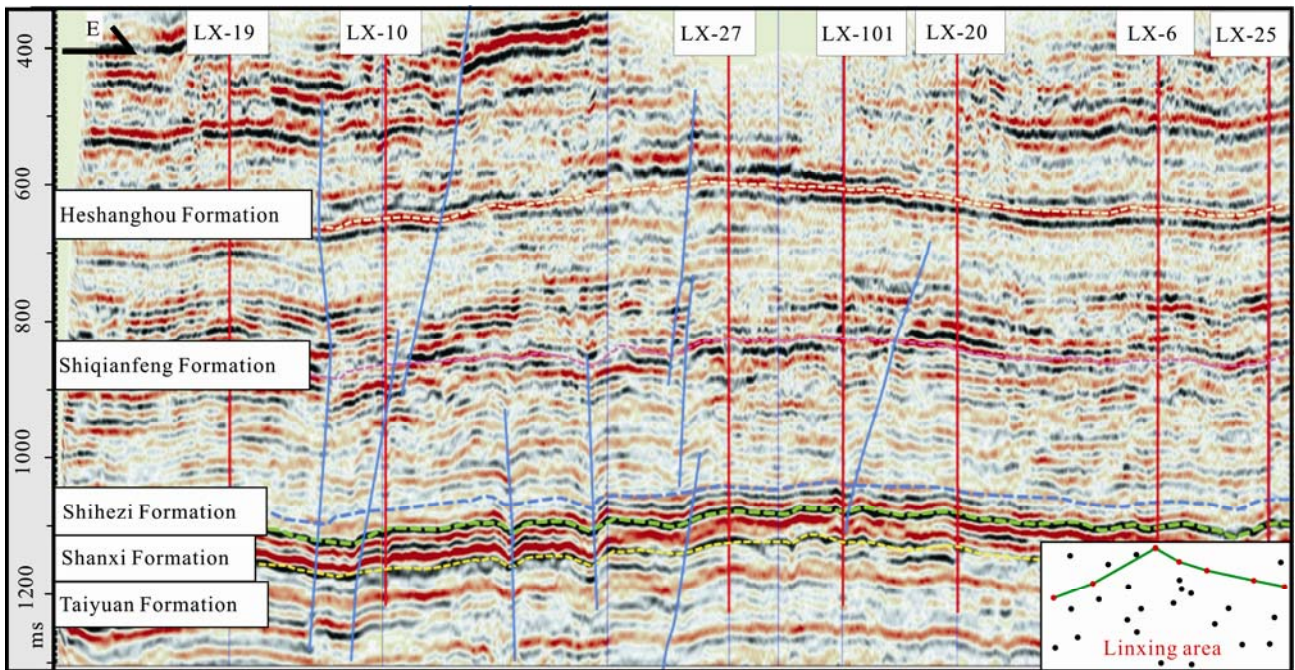


Fig. 19. Faults connecting different formations recognized from seismic section in north of the study area.

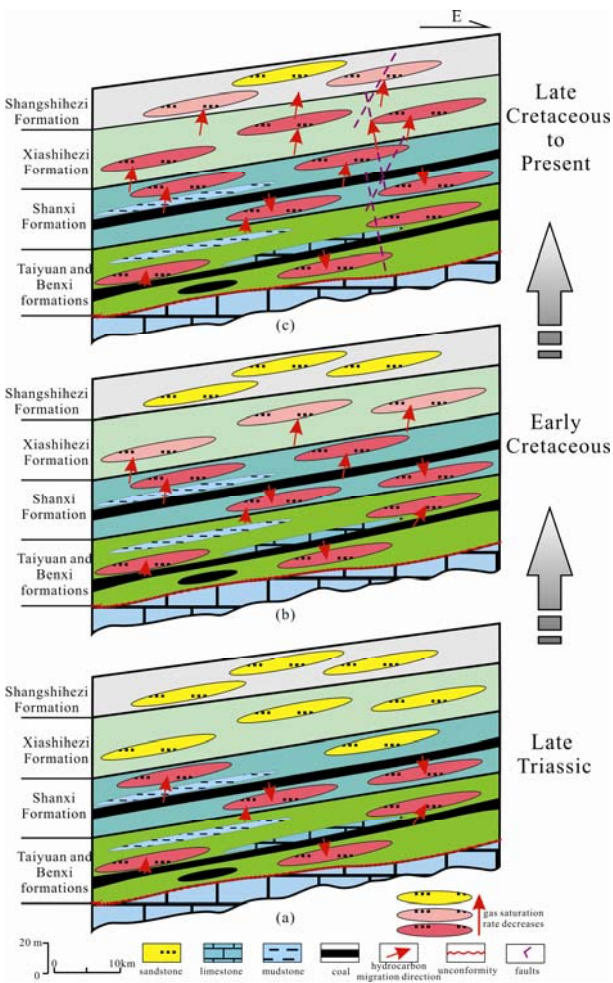


Fig. 20. The gas saturation process in geological history of the study area.

Kong and Macao (grant No. 41728005). We would like to thank Dr. Willem Langenberg for his careful revision and good suggestions for improving the original manuscript.

Manuscript received Sept. 10, 2018
 accepted Nov. 27, 2018
 associate EIC HAO Ziguo
 edited by HAO Qingqing

References

Baioumy, H.M., and Ismael, I.S., 2010. Factors controlling the compositional variations among the marine and non-marine black shales from Egypt. *International Journal of Coal Geology*, 83(1): 35–45.

Barrett, E.P., Joyner, L.S., and Halenda, P.P., 1951. The determination of pore volume and area distributions in porous substances. I. Computations from nitrogen isotherms. *Journal of America Chemistry Society*, 73: 373–380.

Bell, J.S., 2006. In-situ stress and coal bed methane potential in Western Canada. *Bulletin of Canada Petrology Geology*, 54 (3): 197–220.

Bustin, R., and Clarkson, C., 1998. Geological controls on coalbed methane reservoir capacity and gas content. *International Journal of Coal Geology*, 38(1–2): 3–26.

Fall, A., Eichhubl, P., Bodnar, R.J., Laubach, S.E., and Davis, J.S., 2014. Natural hydraulic fracturing of tight-gas sandstone reservoirs, Piceance Basin, Colorado. *Geological Society of America Bulletin*, 127(1–2): 61–75.

Fang Huihuang, Sang Shuxun, Wang Jilin, Liu Shiqi and Ju Wei, 2017. Simulation of Paleotectonic stress fields and distribution prediction of Tectonic fractures at the Hudi Coal Mine, Qinshui Basin. *Acta Geologica Sinica (English Edition)*, 91 (6): 2007–2023.

Flores, R.M., 2014. *Coal and coalbed gas: fuelling the future*. Amsterdam: Elsevier Science: 1–697.

Galloway, B.J., 2016. Geological and geochemical data from the Canadian Arctic Islands. Part XIV: Compilation of rock-eval/TOC and mineralogical data from upper Paleozoic strata of the Sverdrup Basin. *Geol. Surv. Can.* 1–26 Open File 8154.

Gao, X. D., Wang, Y. B., Ni, X. M., Li, Y., Wu, X., Zhao, S. H., and Yu, Y., 2018. Recovery of tectonic traces and its

- influence on coalbed methane reservoirs: A case study in the Linxing area, eastern Ordos Basin, China. *Journal of Natural Gas Science and Engineering*, 56: 414–427.
- Gong, D., Li, J., Ablimit, I., He, W., Lu, S., Liu, D., and Fang, C., 2018. Geochemical characteristics of natural gases related to Late Paleozoic coal measures in China. *Marine and Petroleum Geology*, 96: 474–500.
- Gunter, W.D., Gentzis, T., Rottenfusser, B.A., and Richardson, R.J.H., 1997. Deep coalbed methane in Alberta, Canada: a fuel resource with the potential of zero greenhouse gas emissions. *Energy Conversion and Management*, 38: 217–222.
- Han Hui, Liu Pengwei, Ding Zhengang, Shi Pitong, Jia Jianchao, Zhang Wei, Liu Yan, Chen Shijia, Lu Jungang, Chen Kang, Peng Xudong, Wang Zhiyong, Xiao Shuqi and Gao Yuan, 2018. The influence of extractable organic matter on pore development in the Late Triassic Chang 7 Lacustrine Shales, Yanchang Formation, Ordos Basin, China. *Acta Geologica Sinica* (English Edition), 92(4): 1508–1522.
- Hazra, B., Dutta, S., and Kumar, S., 2016. TOC calculation of organic matter rich sediments using Rock-Eval pyrolysis: Critical consideration and insights. *International Journal of Coal Geology*, 169: 106–115.
- Hakimi, M.H., and Ahmed, A.F., 2016. Organic-geochemistry characterization of the Paleogene to Neogene source rocks in the Sayhut subbasin, Gulf of Aden Basin, with emphasis on organic matter input and petroleum generation potential. *AAPG Bulletin*, 100: 1749–1774.
- Hu, G., Li, J., Shan, X., and Han, Z., 2010. The origin of natural gas and the hydrocarbon charging history of the Yulin gas field in the Ordos Basin, China. *International Journal of Coal Geology*, 81(4): 381–391.
- Hunt, J.M., 1991. Generation of gas and oil from coal and other terrestrial organic matter. *Organic Geochemistry*, 17: 673–680.
- Jiao Yangquan, Wu Liqun, Rong Hui, Peng Yunbiao, Miao Aisheng and Wang Xiaoming, 2016. The relationship between Jurassic coal measures and sandstone-type uranium deposits in the northeastern Ordos Basin, China. *Acta Geologica Sinica* (English Edition), 90(6): 2117–2132.
- Johnson, R.C., and Flores, R.M., 1998. Developmental geology of coalbed methane from shallow to deep in Rocky Mountain basins and in Cook Inlet–Matanuska Basin, Alaska, U.S.A. and Canada. *International Journal of Coal Geology*, 35: 241–282.
- Kang Yongshang, Sun Liangzhong, Zhang Bing, Gu Jiaoyang, Ye Jianping, Jiang Shanyu, Wang Jin and Mao Delei, 2017. The controlling factors of coalbed reservoir permeability and CBM development strategy in China. *Geological Review*, 63 (5): 1041–1418 (in Chinese with English abstract).
- Li Yong, Tang Dazhen, Fang Yi, Xu Hao and Meng Yanjun, 2014. Distribution and genesis of stable carbon isotope in coalbed methane from the east margin of Ordos Basin. *Science China: Earth Sciences*, 57(8): 1741–1748.
- Li Yong and Tang Dazhen, 2015. Deep coalbed methane development in eastern Ordos Basin, China. *Acta Geologica Sinica* (English Edition), 89(s1): 403–404.
- Li Y., Tang D., Xu H., and Meng Y., 2015. Geological and hydrological controls on water co-produced with coalbed methane in Liulin, Eastern Ordos Basin, China. *AAPG Bulletin*, 99(2): 207–229.
- Li, Y., Tang, D., Wu, P., Niu, X., Wang, K., Qiao, P., and Wang, Z., 2016. Continuous unconventional natural gas accumulations of Carboniferous-Permian coal-bearing strata in the Linxing area, Northeastern Ordos Basin, China. *Journal of Natural Gas Science and Engineering*, 36: 314–327.
- Li, Y., Zhang, C., Tang, D., Gan, Q., Niu, X., and Shen, R., 2017. Coal pore size distributions controlled by the coalification process: an experimental study of coals from the Junggar, Ordos, and Qinshui basins in China. *Fuel*, 206: 352–363.
- Liao Jianbo, Xi Aihua, Li Zhiyong, Liu Huaqing, Li Xiangbo and Rong Wanyan, 2018. Microscopic characterization and formation mechanisms of deepwater sandy-debris-flow and turbidity-current sandstones in a lacustrine basin: a case study in the Yanchang Formation of the Ordos Basin, China. *Petroleum Science*, 15: 28–40.
- Lü, D., Chen, J., Li, Z., Zheng, G., Song, C., Liu, H., Meng, Y., and Wang, D., 2014. Controlling factors, accumulation model and target zone prediction of the Coal-bed Methane in the Huanghebei Coalfield, North China. *Resource Geology*, 64(4): 332–345.
- Ma, X., Song, Y., Liu, S., Jiang, L., and Hong, F., 2016. Experimental study on history of methane adsorption capacity of Carboniferous-Permian coal in Ordos Basin, China. *Fuel*, 184: 10–17.
- Magoon, L.B., and Dow, W.G., 1994. The petroleum system – from source to trap. *AAPG Memoir*, 60: 1–655.
- Meng, S., Li, Y., Wang, L., Wang, K., and Pan, Z., 2018. A mathematical model for gas and water production from overlapping fractured coalbed methane and tight gas reservoirs. *Journal of Petroleum Science and Engineering*, 171: 959–973.
- Pan, Z., and Connell, L.D., 2012. Modelling permeability for coal reservoirs: A review of analytical models and testing data. *International Journal of Coal Geology*, 92: 1–44.
- Pashin J.C., 2010. Variable gas saturation in coalbed methane reservoirs of the Black Warrior Basin: implications for exploration and production. *International Journal of Coal Geology*, 82: 135–146.
- Pependic, S.L., Downs, K.R., Vo, K.D., Hamilton, S.K., Dawson, G.K.W., and Golding, S.D., 2011. Biogenic methane potential for Surat Basin, Queensland coal seams. *International Journal of Coal Geology*, 88: 123–134.
- Shuai, Y., Zhang, S., Mi, J., Gong, S., Yuan, X. Yuan, X., Yang, Z., Liu, J., and Cai, D., 2013. Charging time of tight gas in the Upper Paleozoic of the Ordos Basin, Central China. *Organic Geochemistry*, 64(6): 38–46.
- Sykes, R., and Snowdon, L.R., 2002. Guidelines for assessing the petroleum potential of coaly source rocks using rock-eval pyrolysis. *Organic Geochemistry*, 33(12): 1441–1455.
- Su, X., Zhang, L., and Zhang, R., 2003. The abnormal pressure regime of the Pennsylvanian No. 8 coalbed methane reservoir in Liulin–Wupu district, eastern Ordos Basin, China. *International Journal of Coal Geology*, 53(4): 227–239.
- Tonnsen, R.R., and Miskimins, J.L., 2010. A conventional look at an unconventional reservoir: coalbed methane production potential in deep environments. *AAPG Annual Convention and Exhibition in New Orleans, Louisiana*, Poster, 1–2.
- Unsworth, J.F., Fowler, C.S., and Jones, L.F., 1989. Moisture in coal: 2. Maceral effects on pore structure. *Fuel*, 68(1): 18–26.
- Waechter, N.B., Hampton, G. L., and Shipps, J. C., 2004. Overview of coal and shale gas measurement: field and laboratory procedures. *International Coalbed Methane Symposium* University of Alabama, Tuscaloosa, Alabama.
- Wang, W., Zhang, Y., and Zhao, J., 2018. Evolution of formation pressure and accumulation of natural gas in the Upper Palaeozoic, Eastern - central Ordos Basin, Central China. *Geological Journal*, 53(S2): 395–404.
- Wang Shuangming, 2011. Ordos Basin tectonic evolution and structural control of coal. *Geological Bulletin of China*, 30(4): 544–552 (in Chinese with English abstract).
- Wang Yue and Chen Shiyue, 2016. Meandering river sand body architecture and heterogeneity: A case study of Permian meandering river outcrop in Palougou, Baode, Shanxi Province. *Petroleum Exploration and Development*, 43(2): 230–240.
- Wang, M., Li, Z., Huang, W., Yang, J., and Xue, H., 2015. Coal pyrolysis characteristics by TG–MS and its late gas generation potential. *Fuel*, 156: 243–253.
- Wang Tong, Wang Qingwei, Shao Longyi, Xia Yucheng, Fu Xuehai, Ning Shuzheng, Xie Zhiqing and Jiang Tao, 2016. Current status of the research on coal geology in China. *Acta Geologica Sinica* (English edition), 90(4): 1284–1297.
- Wang Zhenliang and Chen Heli, 2007. The distribution and evolution of fluid pressure and its influence on natural gas accumulation in the upper Paleozoic of Shenmu-Yulin area, Ordos Basin. *Science in China* (Earth Sciences), 50: 59–74.
- Wu, H., Ji, Y., Liu, R., and Chen, S., 2018. Pore structure and fractal characteristics of a tight gas sandstone: a case study of

- Sulige area in the Ordos Basin, China. *Energy Exploration & Exploitation*, 5: 1–23.
- Xu, H., Tang, D., Zhao, J., Tao, S., Li, S., and Fang, Y., 2015. Geologic controls of the production of coalbed methane in the Hancheng area, Southeastern Ordos Basin. *Journal of Natural Gas Science and Engineering*, 26: 156–162.
- Xu, H., Tang, D., Zhang, J., Yin, W., Zhang, W., and Lin, W., 2011. Factors affecting the development of the pressure differential in Upper Paleozoic gas reservoirs in the Sulige and Yulin areas of the Ordos Basin, China. *International Journal of Coal Geology*, 85(1): 103–111.
- Yang Hua, Fu Jinhua, Liu Xinshe, Meng Peilong, 2012. Accumulation conditions and exploration and development of tight gas in the Upper Paleozoic of the Ordos Basin. *Petroleum Exploration and Development*, 39(3): 315–324.
- Yang, Y., Li, W., and Ma, L., 2005. Tectonic and stratigraphic controls of hydrocarbon systems in the Ordos Basin: A multicycle cratonic basin in Central China. *AAPG Bulletin*, 89 (2): 255–269.
- Yang, Z., He, S., Guo, X., Li, Q., Chen, Z., and Zhao, Y., 2016. Formation of low permeability reservoirs and gas accumulation process in the Daniudi Gas Field, Northeast Ordos Basin, China. *Marine & Petroleum Geology*, 70(17): 222–236.
- Yang Minghui, Liu Chiyang, Lan Chaoli, Liu Le, Li Xin and Zhang Kunshan, 2010. Late Carboniferous - Early Permian sequence stratigraphy and depositional evolution in the Northeast Ordos Basin, North China. *Acta Geologica Sinica (English Edition)*, 84: 1220–1228.
- Yao, Y., Liu, D., and Yan, T., 2014. Geological and hydrogeological controls on the accumulation of coalbed methane in the Weibei field, southeastern Ordos Basin. *International Journal of Coal Geology*, 121(1): 148–159.
- Zhang, E., Hill, R. J., Katz, B. J., and Tang, Y., 2008. Modelling of gas generation from the Cameo coal zone in the Piceance Basin, Colorado. *AAPG Bulletin*, 92: 1077–1106.
- Zhang, S., Tang, S., Qian, Z., Pan, Z., and Guo, Q., 2014. Evaluation of geological features for deep coalbed methane reservoirs in the Dacheng Salient, Jizhong Depression, China. *International Journal of Coal Geology*, 133: 60–71.
- Zhao Wentao and Hou Guiting, 2017. Fracture prediction in the tight-oil reservoirs of the Triassic Yanchang Formation in the Ordos Basin, northern China. *Petroleum Science*, 14: 1–23.
- Zou Caineng, Tao Shizhen, Han Wenxue, Zhao Zhenyu, Ma Weijiao, Li Changwei, Bai Bin and Gao Xiaohui, 2018. Geological and geochemical characteristics and exploration prospect of coal-derived tight sandstone gas in China: case study of the Ordos, Sichuan, and Tarim Basins. *Acta Geologica Sinica (English Edition)*, 92(4): 1609–1626.

About the first author



LI Yong, male, born in Weifang, Shandong Province, Ph.D., College of Geosciences and Surveying Engineering, China University of Mining and Technology, Beijing, People's Republic of China, is now an associate professor in petroleum and natural gas geology. His interests are sedimentology, reservoirs characterization, and issues associated with unconventional hydrocarbons including coalbed methane, tight gas, shale gas, and gas hydrate. E-mail: liyong@cumtb.edu.cn.